

RECENT RESULTS OF EXPERIMENTS AT VEPP-2M

V. Sidorov  
 Institute of Nuclear Physics  
 Novosibirsk, U.S.S.R.

Summary

During the four years from the end of 1974 up to 1978 a number of experiments were performed at the storage ring VEPP-2M with the detector "OLYA" over the entire energy range covered by VEPP-2M.<sup>1,2</sup> The last season (for OLYA), autumn 1977-summer 1978, was the most productive as far as the integrated luminosity was concerned. At this point the second stage of "OLYA" had been completed (shower and range chambers). All this allowed one to improve the statistical accuracy of the experiments. The integrated luminosity collected during the last measurement cycle was about  $2500 \text{ nb}^{-1}$ . Up to now slightly more than a half of the experimental information has been treated.

Detector "OLYA" and Data Taking

The detector consists of four identical quadrants surrounding the interaction region (Fig. 1). The total solid angle is  $0.65 \times 4\pi$ . Each quadrant contains scintillation triggering counters, time-of-flight counters,

coordinate chambers, a shower detector, and a range system.

In total, the detector contains 32 scintillation counters and 72 planes of spark chambers with ferrite core memory.

The time-of-flight system has a distance between counters of 60 cm (2 nsec) and a resolution time of  $\sigma = 0.25 \text{ nsec}$ . Fast selection by time-of-flight is performed for "collinear" triggering only, allowing one to decrease the detector triggering rate due to cosmic rays by a factor of more than 10. Synchronization of the detector triggering with the time of beam collision provides additional suppression of the cosmic background. Also, the time between counter triggering and beam collision is measured. This information is later used for selection of slow particles (kaons).

Quantitative characteristics of the experiments are presented in Table 1.

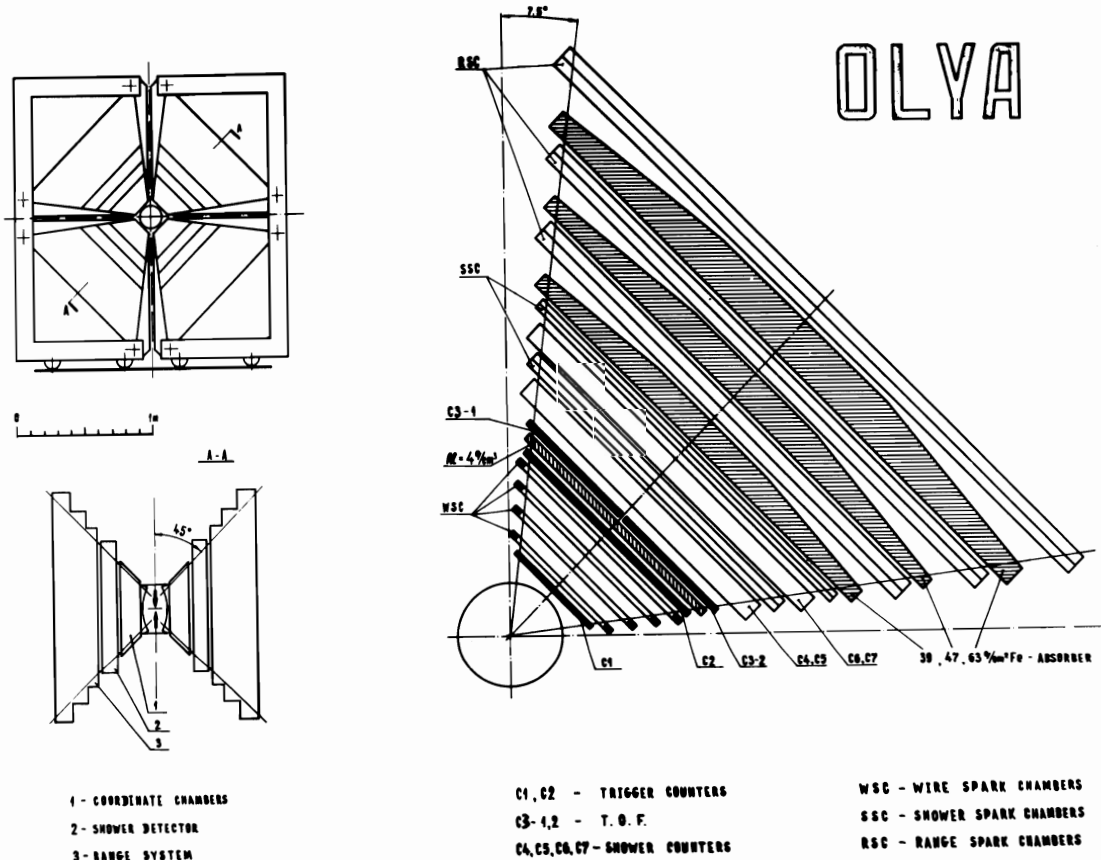


Figure 1. The Detector "OLYA"

2E, GeV	Step (2E), MeV	$\text{nb}^{-1}$	Measurement time, $10^6 \text{ sec}$	Number of triggering $10^6$
1. 0.40 - 0.44	-	3.3	0.47	0.07
2. 1.008 - 1.046	0.5	900.	1.4	1.9
3. 0.64 - 1.00	0.5	800.	2.1	3.1
1.00 - 1.40	0.66	700.	1.0	1.3

Measurement of the pion form factor near the production threshold was made at  $2E = 0.4$  and  $0.44$  GeV, the integrated luminosity at these points being  $2.6 \text{ nb}^{-1}$  and  $0.7 \text{ nb}^{-1}$  respectively, One should note that, despite the low energy, the luminosity of the storage ring was rather good. For example, at  $2E = 0.4$  GeV, luminosity averaged over the measurement time was  $0.6 \times 10^{28}$ , while at  $2E = 0.44$  GeV,  $L = 1.3 \times 10^{28} \text{ cm}^{-2} \text{ sec}^{-1}$ . The maximum luminosity detected during the low energy operation was  $4.5 \times 10^{28} \text{ cm}^{-2} \text{ sec}^{-1}$ .

The second experiment - search for decay of  $\phi \rightarrow \pi^+\pi^-$  - was performed by scanning of the  $\phi$ -meson energy range with a step  $\Delta(2E) = 0.5$  MeV approximately equal to a c.m. energy spread. This experiment consisted of four independent measurement cycles.

The third experiment consisted of scanning the energy range  $0.64 < 2E < 1.4$  GeV. The maximum achieved luminosity was  $3 \times 10^{30} \text{ cm}^{-2} \text{ sec}^{-1}$ .

The luminosity monitoring used the events of the double Bremsstrahlung process. The exact value of the luminosity was calculated by the elastic (Bhabha)  $e^+e^-$  scattering inside the detector solid angle.

The detection efficiencies of the processes under investigation were calculated by the detailed Monte Carlo simulation of the angular distribution and interactions of produced particles.

#### Particle Identification

An essential part of the data treatment consisted in the particle identification of collinear events due to four processes:

$$e^+e^- \rightarrow e^+e^-, \mu^+\mu^-, \pi^+\pi^-, K^+K^-.$$

We traditionally use the correlation matrix method for separation of collinear events.<sup>3</sup> The method is based on a natural assumption that both particles in collinear events belong to a single type. In this case, the two-dimensional spectrum of events (versus any parameters of the two particles) is the overlap of factorized distributions:

$$N(L_1, L_2) = \sum_i N_i P_i(L_1) P_i(L_2).$$

The method gives good results when collinear events contain two types of particles or two groups of particles with similar characteristics. For example, in the separation of events due to the process  $e^+e^- \rightarrow K^+K^-$ , all collinear events were divided into those containing particles with large ionization losses ( $K^+K^-$ ) and those containing minimum ionization particles ( $e^+e^-, \mu^+\mu^-, \pi^+\pi^-$ ).

Practically always the ratio of likelihood functions for pulse heights in scintillation counters was used as an L parameter (in general, L may be calculated by using any particle characteristic).

#### $e^+e^- \rightarrow \pi^+\pi^-$ near threshold

Measurements were performed at two values of energy:  $2E = 0.4$  and  $0.44$  GeV. At these energies, the pion velocity is considerably less than 1. Therefore, separation of collinear events in  $\pi^+\pi^-$  and  $(e + \mu)$  was performed by measuring ionization losses in the first three scintillation counters (C1, C2, C3) and using the correlation matrix method. Fig. 2 shows the existing experimental data on the pion form factor both in the timelike and spacelike regions at small values of  $q^2$ . Also given is the expected value of the pion form factor calculated by the Gounaris-Sakurai formula.<sup>4</sup>

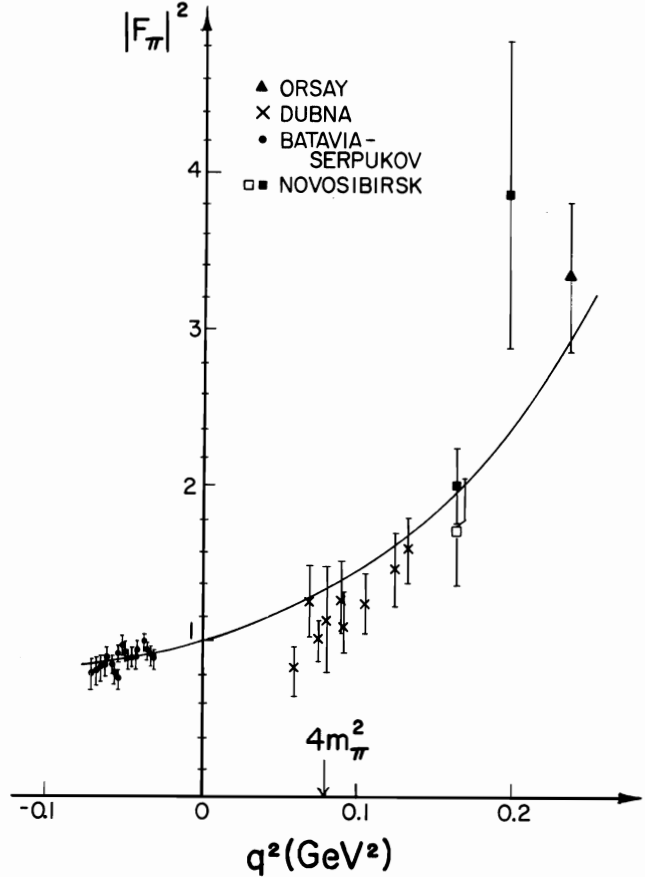


Fig. 2 Data on  $|F_\pi|^2$  in timelike and spacelike regions at small  $q^2$

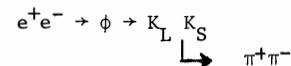
The experimental value of the form factor at  $0.4$  GeV is in good agreement both with theory predictions and the results of another experiment<sup>5</sup> performed at VEPP-2M by Dr. Yu. N. Pestov (in this experiment a time-of-flight detector based on spark counters with localized discharge - Pestov counters - was used). The form factor value obtained at  $0.44$  GeV is about 1.5 standard deviations higher than the theoretical curve.

#### The decay $\phi \rightarrow \pi^+\pi^-$

This decay has not yet been observed. The best upper limit on the branching ratio,  $\beta(\phi \rightarrow \pi\pi) < 2.7 \times 10^{-4}$  (95% C.L.), was obtained.<sup>6</sup> Our previous result was  $B_\pi < 6 \times 10^{-4}$ .<sup>7</sup> The data processing of the new experiment is not finished yet. Up to now, three of four measurement cycles have been analyzed in the narrow energy region around the  $\phi$ -meson ( $m_\phi \pm 10$  MeV).

During the processing, events of three reactions were selected:  $e^+e^- \rightarrow e^+e^-, \mu^+\mu^-, \pi^+\pi^-$ . The charged kaons from  $e^+e^- \rightarrow K^+K^-$  in the  $\phi$ -region have small kinetic energy and do not trigger the system.

The main background to  $e^+e^- \rightarrow \pi^+\pi^-$  comes, in our case, from



For events satisfying the collinearity criteria ( $|\Delta\phi| < 3^\circ$   $|\Delta\phi| < 2^\circ$ ), this process gives at  $\phi$ -maximum

about 2.5% of all  $e^+e^- \rightarrow \pi^+\pi^-$ . But the pions coming from  $K_S$  decays have a characteristic kinematic feature: the energy of one of the pions is close to the minimum possible ( $E = 210$  MeV). Such a pion stops in the shower detector and produces no signal in the subsequent shower and range chambers. Therefore, it was additionally required that for both particles there be at least one spark in the shower/range chambers along the track direction. This cut eliminated about 25% of the main  $\pi^+\pi^-$  effect, but the  $K_S \rightarrow \pi^+\pi^-$  contamination went down to  $\sim 0.1\%$ .

Other processes also give small contamination

$$e^+e^- \rightarrow \phi \rightarrow \pi^+\pi^-\pi^0 < .2\%$$

$$e^+e^- \rightarrow e^+e^- + e^+e^- < .5\%$$

The cosmic background admixture is also negligible.

The cross-section for the reaction  $e^+e^- \rightarrow m^+m^-$ , where  $m = \text{muon or pion}$ , may be written with a  $\phi$ -meson contribution in the form

$$\sigma_{mm}(e) = \sigma_{mm}^0(e) \cdot \left| 1 + \frac{\sigma_\phi B_m}{\sqrt{\sigma_{mm}^0(m_\phi/2)}} e^{i\psi} \frac{m_\phi \Gamma_\phi}{4E^2 - m_\phi^2 + im_\phi \Gamma_\phi} \right|^2.$$

Here,  $E$  is the beam energy,  $m_\phi$  and  $\Gamma_\phi$  are the  $\phi$ -meson mass and width,  $\sigma_\phi$  is the cross-section for production of the  $\phi$ -meson by  $e^+e^-$ ,  $B_m$  is the branching ratio for the decay  $\phi \rightarrow m^+m^-$ ,  $\psi$  is the phase, and  $\sigma_{mm}^0$  is the non-resonant cross-section.

The radiative corrections lead to

$$\sigma_{mm}(E) \rightarrow \sigma_{mm}(\sqrt{E(E-E_\gamma)}) P(E_1 E_\gamma) dE_\gamma,$$

where  $P(E_1 E_\gamma) =$  the emission probability for a photon with energy  $E_\gamma$ . The expression for  $P(E_1 E_\gamma)$ , to double logarithmic accuracy, was taken from Reference 8.

Experimental values for  $N_{\mu\mu}/N_{ee}$  and  $N_{\pi\pi}/N_{ee}$  are given in Fig. 3b and 3c respectively, together with the best fit curves. As an example, Fig. 3a shows the  $\phi$ -meson excitation curve used for energy scale calibration for one scanning cycle.

In fitting the process  $e^+e^- \rightarrow \mu^+\mu^-$  we fixed  $\psi=0$  and  $B_e = (3.1 \pm 0.1) \times 10^{-4}$ . We obtained the result

$$B(\phi \rightarrow \mu\mu) = (4.5 \pm 1.0) \times 10^{-4},$$

which does not contradict the equality  $B_\mu = B_e$ .

The fit for  $\pi^+\pi^-$  interference gave

$$B(\phi \rightarrow \pi\pi) = (1.0 \begin{smallmatrix} +.8 \\ -.5 \end{smallmatrix}) \times 10^{-4}$$

$$\psi = -13^\circ \pm 20^\circ$$

The minimum  $\chi^2$  is 20.5 for 15 degrees of freedom (Fig. 4). For  $B_\pi = 0$  the  $\chi^2$  is 9 units larger than for optimal  $B_\pi$ . This shows that the optimal  $B_\pi$  is at a distance of three standard deviations from zero. In other words, the probability of such a fluctuation for  $B_\pi = 0$  is of the order of  $10^{-3}$ . The latter statement was checked by special Monte Carlo simulation. The optimal form factor for  $B_\pi = 0$  is shown in Fig. 3c by a dashed line.

#### $e^+e^- \rightarrow \pi^+\pi^-$ Measurement of the Pion Form Factor

About one half of the experimental information has been treated covering the c.m. energy range from 1.06 GeV up to 1.40 GeV.<sup>12</sup> The admixture of events due to  $e^+e^- \rightarrow K^+K^-$  in collinear events was decreased to 1% by a procedure developed for selection of  $K^+K^-$  events

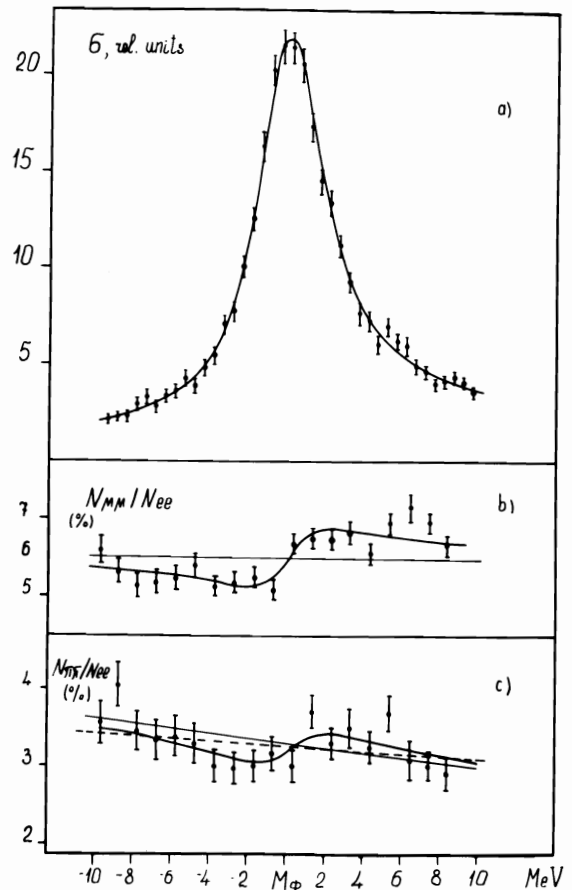


Fig. 3 a) The excitation curve of the  $\phi$ -meson used for calibration of the energy scale in one scanning cycle.

b) The experimental values for  $N_{\mu\mu}/N_{ee}$  and the best fit curve.

c) The same for  $N_{\pi\pi}/N_{ee}$ . The solid straight line is the form factor for optimal  $B_\pi$ , the dashed one is the optimal form factor for  $B_\pi = 0$ .

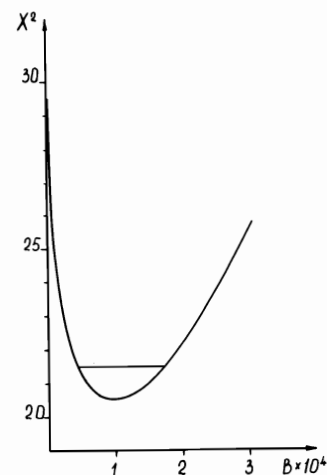


Fig. 4 The  $\chi^2$  versus  $B_\pi$

$$\Delta\chi^2(B_\pi = 0) = 9$$

based on pulse heights in triggering counters (see the next section). Separation of three types of events with minimum ionization particles was performed by correlation matrix method.

Using the selected  $\mu^+\mu^-$  events we have performed the comparison of the experimental cross section with Q.E.D. predictions. Good agreement ( $\chi^2/n = 22.7/17$ ) provides evidence for the correctness of the separation procedures (Fig. 5).

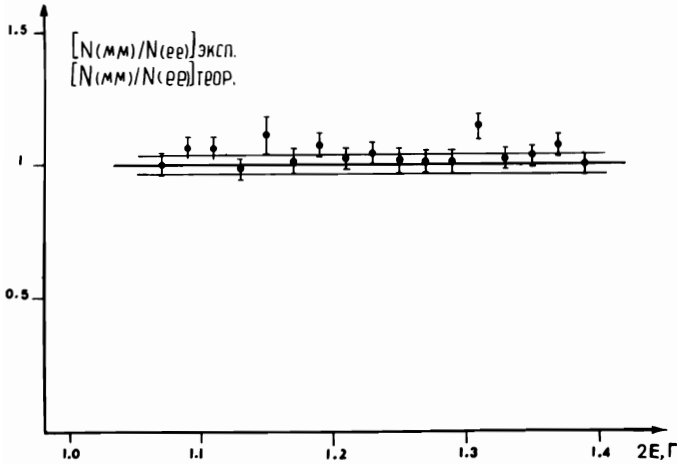


Fig. 5 Energy dependence of  $N_{\mu\mu}/N_{ee}$  normalized to the QED prediction. The statistical error of the Monte Carlo simulation is shown by a corridor.  $\chi^2 = 22.7/17$  corresponding to 16% C.L.

In Figs. 6 and 7 we present the experimental values obtained in the previous works and in this experiment. The solid curve corresponds to the  $\rho$ -meson tail calculated by the Gounaris-Sakurai formula with  $\rho$ - $\omega$  interference taken into account.

Experimental values of  $|F_{\pi}|^2$  are considerably above the curve - the maximum deviation being at 1.2 GeV. At first sight this circumstance supports the existence of the long-discussed  $\rho' \rightarrow \pi^+\pi^-$ . However, such a conclusion is not evident. Experimental data (see below) show the rapid increase of multihadron

cross-sections in this energy range. This must also influence the pion form factor behaviour. The model independent calculations<sup>9</sup> demonstrated that this effect could explain the observed excess. But as it was shown<sup>10</sup>, taking into account inelastic channel contributions can only decrease the pion form factor if vector dominance with only the  $\rho$  (776) is used.

Constructive interference appears if one assumes the existence of the  $\rho'$  (1250) with a peak cross section  $\sim 30$  nb and the dominant decay mode  $\rho' \rightarrow \omega\pi$ .<sup>11</sup> The calculations of  $|F_{\pi}|^2$  made in this work are in qualitative agreement with our results.

$$e^+e^- \rightarrow K^+K^-$$

Events from the process  $e^+e^- \rightarrow K^+K^-$  begin to trigger the detector at  $2E = 1.12$  GeV. The kaon velocity in this energy range is much less than unity, varying from  $\beta = 0.47$  at  $E = 0.56$  to  $\beta = 0.71$  at  $E = 0.70$  GeV. Therefore, selection of these events among all collinear events by the method of correlation matrices is based on large ionization losses in scintillation counters. The total number of selected events is 1375.

Fig. 8 shows the values of  $|F_{K^+}|^2$  obtained in this experiment together with the results of our previous experiment.<sup>2</sup> The curve is the calculation in the vector dominance model with  $\rho$ ,  $\omega$ ,  $\phi$  meson interference into account:

$$F_{K^+} = \frac{1}{2} \frac{m_{\rho}^2}{\Delta_{\rho}} + \left( \frac{1}{2} - \frac{f_{\phi K \bar{K}}}{f_{\phi}} \right) \frac{m_{\omega}^2}{\Delta_{\omega}} + \frac{f_{\phi K \bar{K}}}{f_{\phi}} \frac{m_{\phi}^2}{\Delta_{\phi}},$$

where  $\Delta_{\nu} = m_{\nu}^2 - s - im_{\nu}\Gamma_{\nu}$ , and for the  $\phi$ -meson coupling constants the experimental value is taken:

$$\frac{f_{\phi K \bar{K}}}{f_{\phi}} = .33.$$

For simplicity, finite width corrections are omitted. This results in a 10% inaccuracy in the calculated value of the form factor.

In the whole explored region, experimental values of  $|F_{K^+}|^2$  exceed considerably the predictions of the vector dominance model based on  $\rho$ ,  $\omega$ ,  $\phi$ -mesons. At the maximum energy the ratio of the experimental to theoretical value is 3.

Fig. 6  
 $|F_{\pi}|^2$  versus energy.  
The curve is the Gounaris-Sakurai prediction with the taken into account.

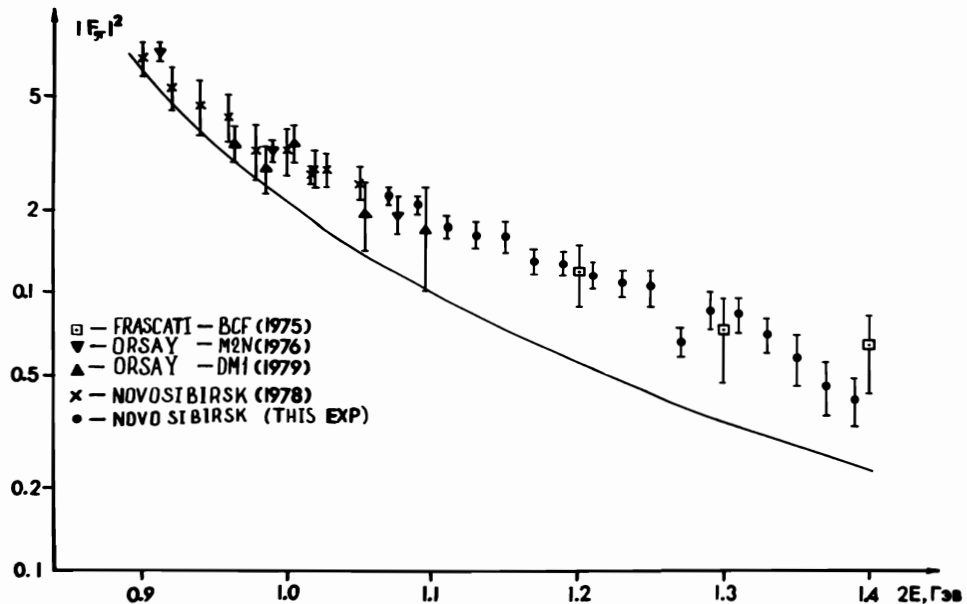


Fig. 7  
 $|F_{\pi}|^2$  versus energy for  
 $0.4 < 2E < 1.4$  GeV.  
 The curve is the  
 Gounaris-Sakurai prediction.

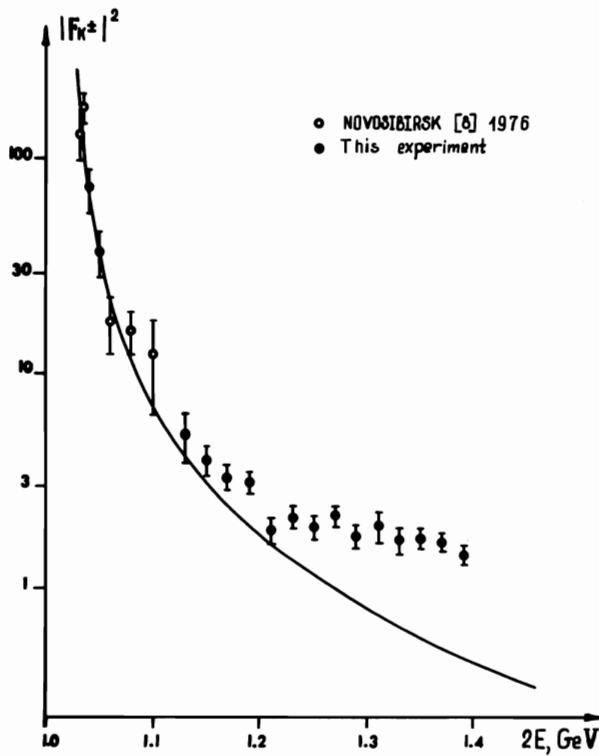
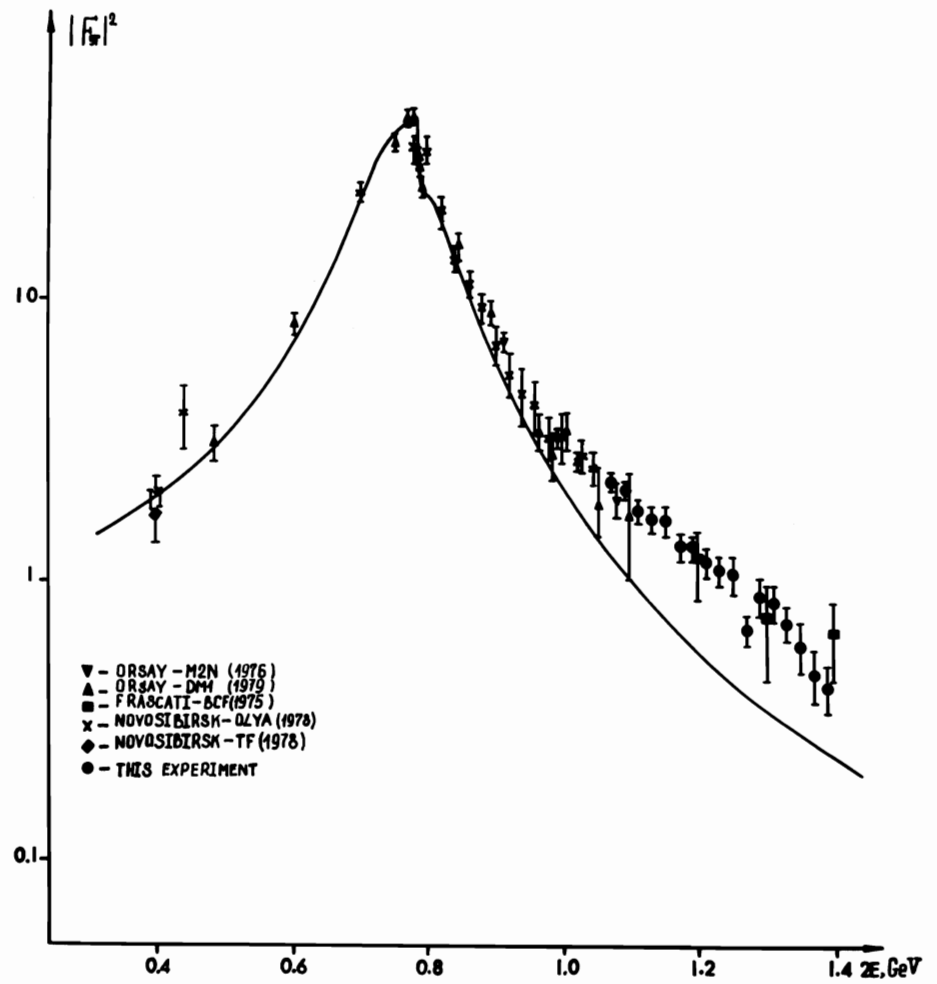


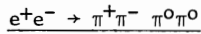
Fig. 8  
 Energy dependence of the  
 charged kaon form factor.  
 The curve is the prediction  
 of vector dominance  
 with  $\rho$ ,  $\omega$  and  $\phi$ -mesons.

As in the case of  $e^+e^- \rightarrow \pi^+\pi^-$ , this can be due to the effect of inelastic channels.<sup>17,19</sup> However, the assumption that inelastic channels give the same contribution to the isovector part of the kaon form factor doesn't provide a quantitative explanation of the observed excess. It is clear that for better understanding of the situation, measurement of a neutral kaon form factor is needed. Knowledge of both  $F_K^+$  and  $F_K^0$  allows one to separate the isoscalar and isovector parts of the kaon form factor.

In Fig. 9 we present all available information on  $|F_K^+|^2$  in the energy region from 1.0 up to 2.2 GeV. Note that recent results from DCI<sup>12</sup> also indicate a considerable excess in  $|F_K^+|^2$  over the simplest vector dominance predictions at  $2E \sim 1.6$  GeV.

If one assumes the energy dependence of  $|F_K^+|^2$  to be given by resonances, then in order to account simultaneously for the smallness of  $|F_K^0|^2$ <sup>12</sup>, one must postulate two resonances. Only in this way can the interference with  $\rho$ ,  $\omega$ , and  $\phi$ -meson tails result in an increase in  $|F_K^+|^2$  without a similar increase in  $|F_K^0|^2$ .

Such a possibility was discussed in References 13 and 14, where four quark resonances (molecules) were predicted with a mass about 1.5 GeV.



To study this reaction, "2ch + n $\gamma$ " events were selected by requiring  $\gamma$ -quanta in shower chambers of the quadrants without tracks. Analysis showed that events with one detected  $\gamma$ -quantum were strongly "contaminated" by the radiative processes like  $e^+e^- \rightarrow e^+e^-\gamma$ . The number of events with four detected  $\gamma$ -quanta was negligibly small. Therefore, only events with 2 or 3  $\gamma$ 's were considered. Analysis of the angular distribution of these events as well as the ratio  $N_{3\gamma}/N_{2\gamma}$  show that at energies higher than that of the  $\phi$ -meson

the contribution of the channel  $\pi^+\pi^-\pi^0$  is small. Thus the observed events are due to the channel  $\pi^+\pi^-\pi^0\pi^0$  in which the  $\omega\pi^0$  intermediate mechanism dominates.

In Fig. 10 the cross section of the process  $e^+e^- \rightarrow \pi^+\pi^-\pi^0\pi^0$  is presented. Also shown are the results of experiments with ACO, DCI, and ADONE. No structures are present in the cross section. It grows with energy, and at  $2E \geq 1.2$  GeV, it exceeds considerably the prediction of the vector dominance model based on  $\rho$  (776)<sup>15,16</sup> (solid curve). The accuracy of this experiment is higher than that in the previous one,<sup>2</sup> the results being consistent.

It is clear that in discussing whether or not the large value of the cross section in the region 1.2 - 1.4 GeV is due to the new resonance ( $\rho'$  (1250)) one should take into account the contribution of  $\rho'$  (1600). In fact, the main mechanism of the decay  $\rho' \rightarrow 2\pi^+ + 2\pi^-$  is through  $\rho\pi^+\pi^-$ . Therefore, by isospin symmetry,  $\rho\pi^0\pi^0$  must contribute to the channel  $e^+e^- \rightarrow \pi^+\pi^-\pi^0\pi^0$ . Isospin conservation leads to the prediction  $\sigma(e^+e^- \rightarrow \rho\pi^+\pi^-)/\sigma(e^+e^- \rightarrow \rho\pi^0\pi^0) = 2$ . However, the interference due to a large  $\rho$ -meson width and identical pions leads<sup>17</sup> to energy dependence of the ratio. It approaches 2 only at very high energy when the  $\rho$ -meson is produced with a large momentum, while in the region 1.2 - 1.6 GeV it is somewhat higher ( $\sim 3$ ). Thus, the contribution of the channel  $2\pi^+ + 2\pi^-$  to the channel  $\pi^+\pi^-\pi^0\pi^0$  is essentially lower than is usually assumed.

The conclusion<sup>18</sup> about the nonexistence of  $\rho'$  (1250) is based essentially on the value of its leptonic width  $\Gamma_{\rho',ee} \sim 4$  KeV. The resulting very large cross section,  $\sigma(e^+e^- \rightarrow \pi^+\pi^-\pi^0\pi^0) \sim 150-250$  nb, is in contradiction with the experiment. On the other hand, data on  $\rho'$  (1250) photoproduction indicate a much lower value:  $\Gamma_{\rho',ee} \sim 0.6$  KeV.<sup>19</sup> This value is in line with the analysis<sup>11</sup> in which  $\rho'$  (1250) with the main decay

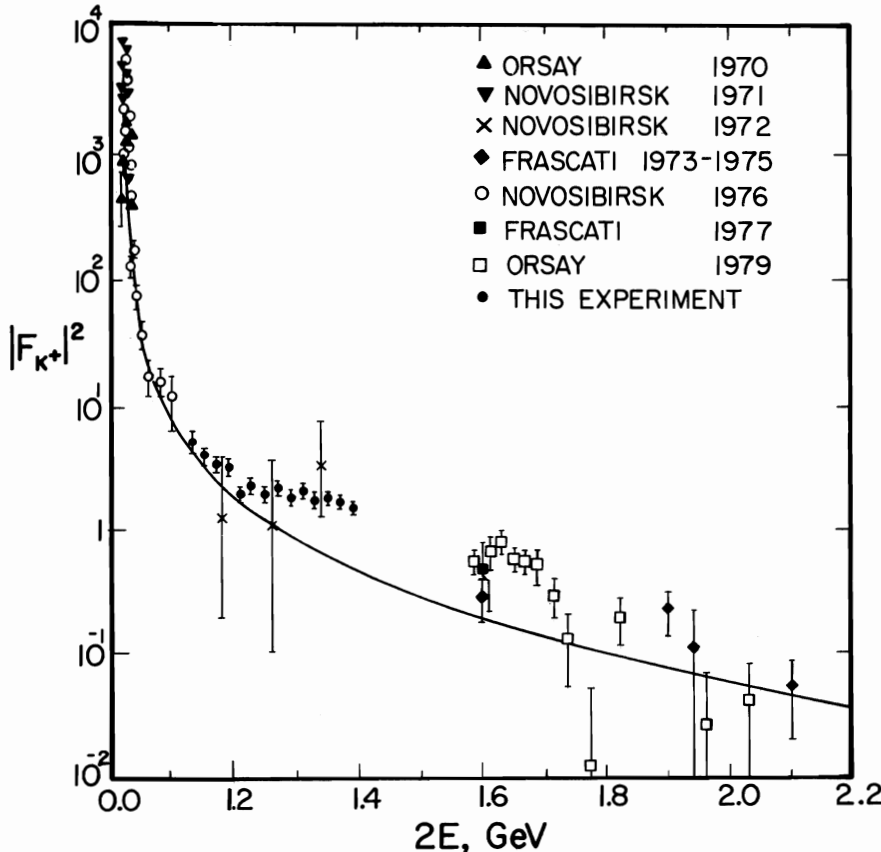


Fig. 9

All data available on  $|F_K^+|^2$  in the energy range  $1 < 2E < 2.2$  GeV. The curve is the prediction of vector dominance with  $\rho, \omega$  and  $\phi$ -mesons.

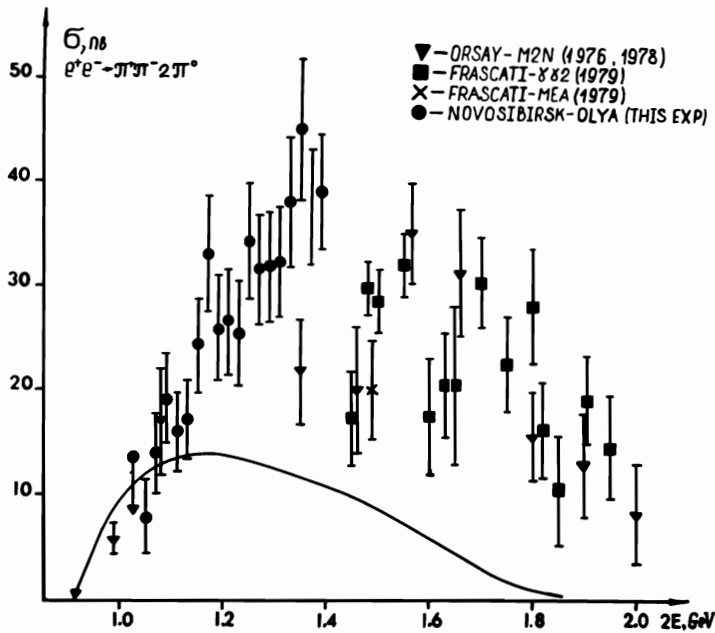
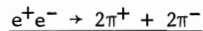


Fig. 10

Cross section of the reaction  $e^+e^- \rightarrow \pi^+\pi^- 2\pi^0$ . Solid curve - a calculation for  $e^+e^- \rightarrow \rho \rightarrow \omega\pi^0$ .

mode  $\omega\pi^0$  is used to describe simultaneously data on  $e^+e^- \rightarrow \pi^+\pi^-\pi^0\pi^0$ . If one assumes that the excess over the  $\rho$ -meson tail is due to  $\rho'$  (1250) only, then  $\Gamma_{\rho,ee} \sim 0.5$  KeV is consistent with References 11 and 19. One concludes that it is too early to make final adjustments. To describe the whole situation in this energy region one must consider simultaneously all the resonances. This problem does not seem very simple from the theoretical point of view. It is clear that experimental separation of different mechanisms ( $\omega\pi^0$ ,  $\rho\pi\pi$ ,  $A$ ,  $\pi$  etc.) will considerably improve our understanding of the problem.



Events with 3 or 4 tracks without  $\gamma$ -quanta were selected. Analysis of pulse height spectra showed that the three- and four-track events are similar. This provided good support for the assumption of their common origin.

Assuming that produced particles are pions from the reaction  $e^+e^- \rightarrow 2\pi^+ + 2\pi^-$ , one can perform complete reconstruction of four-track events, i.e. calculate particle energies by their angles. Then invariant masses of different combinations of pion pairs are obtained (their total number is 6). The corresponding distribution is shown in Fig. 11 for  $1.35 < 2E < 1.40$  GeV. One can clearly see the excess of experimental events over the curve (simulation in the LIPS model) in the vicinity of the  $\rho$ -meson mass. The excess is statistically significant:  $43 \pm 12$  events are observed, i.e. one sees a 3.5 standard deviation effect. This gives evidence for the  $\rho\pi\pi$  mechanism of  $2\pi^+ + 2\pi^-$  production, in agreement with recent observations at Frascati at  $2E \geq 1.5$  GeV.<sup>20</sup> One should note that such a  $\rho$ -meson signal is observed only at the highest attainable energy. This is not surprising if one takes into account strong interference among final states differing by permutations of identical pions.<sup>17</sup> At our energy this effect smears the  $\rho$ -meson peak. Besides that, we do not distinguish between neutral and charged combinations of pion pairs. Therefore, two "charged" combinations are added to the four "neutral" combinations in which the  $\rho$ -meson can be seen.

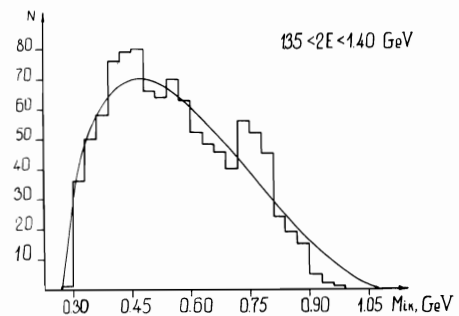


Fig. 11 Distribution in invariant masses of pion pairs,  $1.35 < 2E < 1.40$  GeV. The solid curve is the prediction of phase space (LIPS) model.

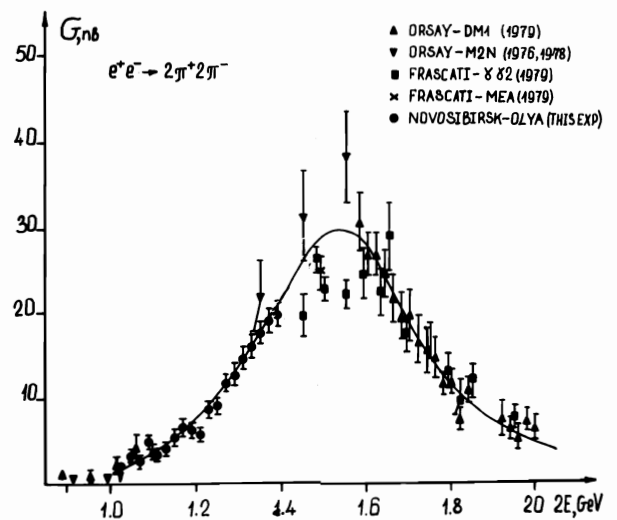


Fig. 12 Cross section of the reaction  $e^+e^- \rightarrow 2\pi^+ 2\pi^-$ . Solid curve - a two resonance fit (interference of  $\rho$  (776) and  $\rho'$  (1600))

In Fig. 12 the cross section of the reaction  $e^+e^- \rightarrow 2\pi^+ + 2\pi^-$  is shown. These results are consistent with our previous experiment,<sup>2</sup> while the accuracy is much better. Also shown are the data from ACO, DCI, and ADONE. The picture indicates a resonance with a mass of about 1.6 GeV. However, in the region 1.1 - 1.2 GeV, a kind of a "shoulder" is observed, which could be due to the interference between  $\rho$  (776) and  $\rho'$  (1600) contributions. The solid curve shown in Fig. 12 is a two-resonance fit ( $\chi^2/h = 29.4/35$ ), which is much better than a one resonance fit ( $\chi^2/h = 50.0/36$ ).

### The Search for Narrow Resonances

The experimental search for new resonances, performed at the storage ring VEPP-2M in 1975<sup>2</sup> showed that there were no new narrow resonances with a large cross section ( $\Gamma(X \rightarrow ee) < 100$  eV) in the energy region 1.0 - 1.34 GeV. However, at about that time one of the DESY groups had seen a cross section energy dependence irregularity interpreted as a resonance at the energy 1100 MeV.<sup>19</sup> In that experiment the value of  $\Gamma(X \rightarrow ee)$  was not measured directly. Also, the main decay modes of the resonance were not known. Thus, it was impossible to predict the result of the colliding beams experiment. In the present experiment, a second attempt was made to find the small resonances with experimental statistics 5 times greater than that of our previous experiment. In the search for resonances, the distributions of events containing  $\pi^+\pi^-$ ,  $K^+K^-$ ,  $\omega\pi^0$ ,  $2\pi^+2\pi^-$  were obtained (Fig. 13) by using the extraction procedure described above.

The partial decay mode to electron-positron pairs is proportional to the area of the resonance ( $\Gamma(V \rightarrow ee) \sim \int \sigma(E)dE$ ). Therefore, estimating the resonance  $\Gamma_{ee}$  upper limit is equivalent to computing the area under the resonance peak for the largest fluctuation consistent with the data.

In spite of some irregularities (especially in the right-hand slope of the  $\phi$ -meson) which do not quite seem to be statistical, we cannot up to now report anything beyond upper limits for a partial width  $\Gamma_{ee}$ . The upper limits, multiplied by the branching ratio B of the decay channel investigated, have been obtained at 90% confidence level under various assumptions about the resonance width and decay channel.

To determine the upper limit for  $B\Gamma_{ee}$ , the corresponding detection efficiencies are needed. In the following table they are presented for the average energy of the interval explored. The variation at the interval ends doesn't exceed 10% of the given values.

Decay Channel	Detection efficiency %	$B\Gamma_{ee}$ - Upper limit (eV)	
		1 MeV	10 MeV
$e^+e^- \rightarrow V \rightarrow \pi^+\pi^-$	38	12	13
$e^+e^- \rightarrow V \rightarrow K^+K^-$	36	5	9
$e^+e^- \rightarrow V \rightarrow \omega\pi^0$	9	22	31
$e^+e^- \rightarrow V \rightarrow 4\pi^\pm$	27	3	13

Thus, in the energy region explored, no narrow resonances ( $\Gamma < 10$  MeV) were observed with a leptonic width greater than 1/40 of that for  $\phi$ -meson.

More detailed descriptions of the experiments are given in the papers listed in References 21 thru 25 submitted to this Symposium.

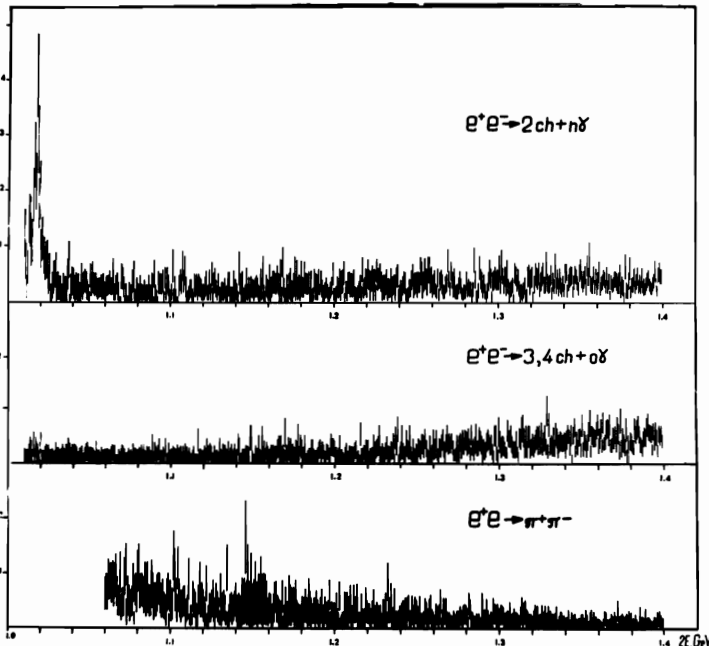


Fig. 13

Experimental energy distribution of events of the processes  $e^+e^- \rightarrow \omega\pi^0$ ,  $2\pi^+2\pi^-$ ,  $\pi^+\pi^-$



## References

1. V.M. Aulchenko et al., Proceedings of the V<sup>th</sup> International Symposium on High Energy Physics, p. 163, Warsaw, 1975.
2. V.A. Sidorov, Proceedings of the XVIII<sup>th</sup> International Conference on High Energy Physics, v. 2, p. B13, Tbilisi, 1976.
3. A.D. Bukin et al., Preprint INP 77-92, Novosibirsk, 1977.
4. G. Gounaris and J. Sakurai, Phys. Rev. Lett 21, (1968) 244.
5. I.B. Vasserman et al., Yadernaya Fizika, 28 (1978) 968.
6. H. Alvensleben et al., Phys. Rev. Lett., 28 (1972) 66.
7. A.D. Bukin et al., Yadernaya Fizika, 27 (1978) 985.
8. G. Parroux et al., Preprint L.A.L. 1280 (1975) Orsay.
9. V.N. Baier and V.S. Fadin, Pis'ma v JETP, 15 (1972) 219.
10. B. Bonneau and F. Martin, Nuovo Cimento 13A (1973) 413.
11. N.M. Budnev et al., Phys. Lett., 70B (1977) 365.
12. B. Delcourt, Present Symposium.
13. R.L. Jaffe, Phys. Rev. D15 (1977) 267, 281.
14. F.E. Close and H.J. Lipkin, Phys. Rev. Lett., 41 (1978) 1263.
15. J. Layssac and F.M. Renard, Nuovo Cimento Lett. 1 (1971) 197.
16. A.M. Altukhov and I.B. Khriplovich, Yadernaya Fizika, 14 (1971) 783.
17. S.I. Eidelman, Pis'ma v JETP, 16 (1977) 563.
18. M. Spinetti, Present Symposium.
19. S. Bartalucci et al., Nuovo Cimento 49A (1979) 207.
20. B. Esposito et al., Nuovo Cimento Lett. 25 (1979) 5.
21. A.D. Bukin et al., Preprint INP 79-66, Novosibirsk, 1979.
22. I.A. Koop et al., Preprint INP 79-67, Novosibirsk, 1979.
23. P.M. Ivanov et al., Preprint INP 79-68, Novosibirsk, 1979.
24. L.M. Kurdadze et al., Preprint INP 79-69, Novosibirsk, 1979.
25. V.M. Aulchenko et al., Preprint INP 79-65, Novosibirsk, 1979.

## Discussion

R. Diebold, Argonne National Laboratory: You say you hope to have luminosity in VEPP-4 by the end of the year. Will the detector also be ready by then? What's the schedule?

V. Sidorov: There are three interaction points at VEPP-4. One detector, namely "OLYA", which has now finished its runs on VEPP-2M, is already in place in one of the interaction points of VEPP-4. The main detector is going to be ready to some extent at the end of this year, but we'll move it into place as late as possible because the detector is being improved.

B. Margolis, McGill University: This is a comment in connection with this paper and those in the last section on photoproduction of vector states in the mass region near 1600 MeV. One should expect two states, perhaps, due to the possibility of having qq in relative  $\ell=0$  and  $\ell=2$  configurations, such as the  $\psi'(3.69)$  and  $\psi''(3.77)$ , which are mixtures of s and d states.

A. Sirlin, New York University: I would like to ask whether you will be able to extract the values for the charged radii of the  $\pi$  meson and K meson. Your people previously got a value for the  $\pi$ .

V. Sidorov: No, there is no such analysis. There is no data on the K, and though there is some additional data on the  $\pi$ , we haven't analyzed it in terms of radius because there are only two points. That's not enough.

Tran N. Truong, Ecole Polytechnique: Does the pion form factor measured in this experiment agree with the earlier measurement at Novosibirsk? This is important in testing CVC in heavy lepton  $\tau$  decay.

V. Sidorov: Yes, the only difference is that the accuracy is better now. It agrees with our previous results.

H. Meyer, University of Wuppertal: What's the peak luminosity at the  $\phi$ -mass?

V. Sidorov: The peak luminosity is  $2 \times 10^{30}$ .

J. Ellis, CERN: Could you quote a number for the ratio of the  $K^+K^-$  and  $\pi^+\pi^-$  form factors at your highest energy?

V. Sidorov: I don't remember the absolute value, but it is about a factor of two in excess of the theory curve for the  $\pi$ 's and about a factor of three in excess for the K's.